

## Aggregation of inertial particles in random flows

B. Mehlig,<sup>1</sup> M. Wilkinson,<sup>2</sup> K. Duncan,<sup>2</sup> T. Weber,<sup>1</sup> and M. Ljunggren<sup>1</sup>

<sup>1</sup>*Department of Physics, Göteborg University, 41296 Göteborg, Sweden*

<sup>2</sup>*Department of Applied Mathematics, The Open University, Walton Hall, Milton Keynes, MK7 6AA, England*

(Received 25 April 2005; published 8 November 2005)

We consider the trajectories of particles suspended in a randomly moving fluid. If the Lyapunov exponent of these trajectories is negative, the paths of these particles coalesce, so that particles aggregate. Here we give a detailed account of a method [B. Mehlig and M. Wilkinson, *Phys. Rev. Lett.* **92**, 250602 (2004)] for calculating this exponent: it is expressed as the expectation value of a random variable evolving under a stochastic differential equation. We analyze this equation in detail in the limit where the correlation time of the velocity field of the fluid is very short, such that the stochastic differential equation is a Langevin equation. We derive an asymptotic perturbation expansion of the Lyapunov exponent for particles suspended in three-dimensional flows in terms of a dimensionless measure of the inertia of the particles,  $\epsilon$ , and a measure of the relative intensities of potential and solenoidal components of the velocity field,  $\Gamma$ . We determine the phase diagram in the  $\epsilon$ - $\Gamma$  plane.

DOI: [10.1103/PhysRevE.72.051104](https://doi.org/10.1103/PhysRevE.72.051104)

PACS number(s): 05.40.-a, 05.60.Cd, 46.65.+g

### I. INTRODUCTION

#### A. Illustration and context

Figure 1 illustrates a simulation of the distribution of small particles suspended in a three-dimensional random flow: the particles are modeled as points, but they are shown as small spheres to make them visible in the figure. The suspended particles do not interact (that is, the motion of each particle is independent of the coordinates of the other particles, the equations of motion are given below). We show the initial configuration [Fig. 1(a)], and two snapshots of the particle positions after a long time, with differing values of the fluid viscosity, [Figs. 1(b) and 1(c)]. In one case the particles aggregate, in the sense that the trajectories of different particles coalesce. In the other case their distribution shows some degree of clustering, but their trajectories never coalesce. In this paper we present an analysis of the transition between aggregating and nonaggregating phases of non-interacting point particles, which we term the path-coalescence transition. We remark that finite-sized particles which combine when they approach within a given radius will eventually aggregate when advected in a mixing flow. This is a different problem, which is not addressed in our paper.

There are numerous experimental observations that when small particles are suspended in a complex and apparently random flow, their density becomes nonuniform. Clustering of particles into regions of high density has been observed in experiments on particles floating on the surface of liquids with a complex or turbulent flow [1,2], and also turbulent flow in channels [3,4]. The conditions under which this occurs are not yet fully understood. The aggregation effect illustrated in Fig. 1 is an extreme form of clustering. There appears to be less experimental work on aggregation, and this process is still not very well understood. In particular it is not clear when a model of point particles suspended in a random flow can exhibit aggregation, and when additional physical phenomena involving the finite size of the particles must be invoked.

Earlier theoretical work on clustering in random flows has used Fokker-Planck equations determining moments of the particle density of advected particles [5]. This passive scalar approach does not allow for the effects of inertia of the particles. It has been supplemented by a perturbative analysis of the deviations of particles from advected trajectories, as proposed by Maxey [6]. These two approaches are combined in Refs. [7,8]. Numerical work indicates that clustering in solenoidal flows occurs most readily when the correlation time of the velocity field is comparable with the time constant associated with the viscous drag [9,10]. The aggregation (as opposed to clustering) of particles by random flows has received relatively little attention. Deutsch [11] appears to have been the first to propose that particles subjected to a smooth random flow can coalesce, and showed numerical evidence that this can happen in one dimension. He argued that there is a transition between coalescing and noncoalescing phases, and identified the dimensionless parameter which determines the phase transition in one dimension.

This paper describes results obtained from an approach to characterizing particle aggregation in random flows. An outline of this method and results for two spatial dimensions have been published previously in a shorter communication [12].

Particles suspended in a randomly moving fluid aggregate if the maximal Lyapunov exponent characterizing the rate of separation of nearby particles is negative. Here we show how to calculate this exponent as the expectation value of one of several random variables evolving under coupled stochastic differential equations. In the limit as the correlation time of the flow approaches zero, the stochastic differential equations can be reduced to a pair of Langevin equations. We give a detailed account of the method and use it to derive results for three-dimensional flows. The corresponding results for one and two spatial dimensions are summarized in Ref. [13] (where we solved Deutsch's one-dimensional model exactly), and in Ref. [12] (two-dimensional case). The three-dimensional case discussed in the following is most

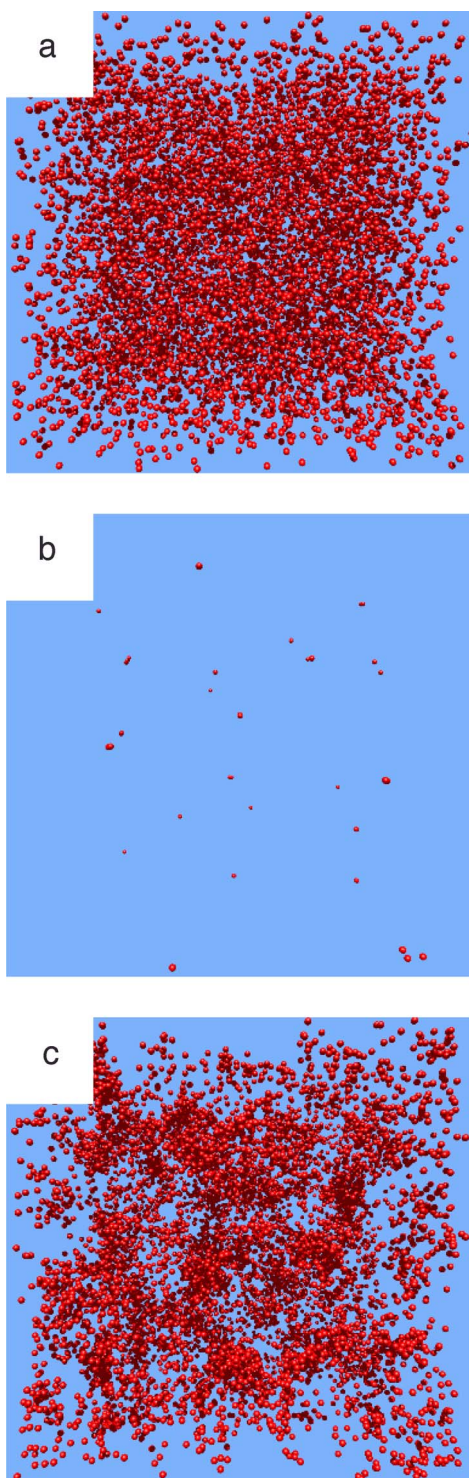


FIG. 1. (Color online) Illustrating the aggregation of noninteracting particles in a random three-dimensional flow, the motion is defined by Eqs. (1)–(3), using a simplified form explained in Sec. III, see Eqs. (41) and (42). Panel (a) shows the initial configuration at  $t=0$ , panels (b) and (c) show configurations after a long time for two different values of  $\gamma$ . In the case shown in the center panel, trajectories coalesce, until eventually all particles follow the same trajectory. The particles in the right panel exhibit density fluctuations, but the trajectories do not coalesce.

important for physical applications, but involves substantial additional technical complications.

We remark that the two-dimensional case was also considered in Ref. [14] where an analytic expression for the maximal Lyapunov exponent was quoted. This expression is incorrect in two dimensions, because the generating function used in deriving the result is divergent for the equilibrium distribution. The calculation can be adapted to give the correct expression in the one-dimensional case, as quoted in Ref. [12].

The definition of Lyapunov exponents is explained in Ref. [15], where the method we use for extracting the Lyapunov exponents from direct numerical simulations is also discussed. We note that in the case where inertia of the particles can be neglected, our results reduce to calculating the Lyapunov exponent for spatially correlated Brownian motion, which was discussed from a mathematical point of view in Ref. [16] and Ref. [17].

### B. The model

The most natural model for theoretical investigation is the motion of spherical particles (radius  $a$ , mass  $m$ ) moving in a random velocity field  $\mathbf{u}(\mathbf{r}, t)$  with specified isotropic and homogeneous statistical properties. The particles are assumed not to affect either the flow, or each other's motion, and to experience a drag force given by Stokes's law: the force  $\mathbf{f}_{\text{dr}}$  on a particle moving with velocity  $\mathbf{v}$  relative to the fluid is  $\mathbf{f}_{\text{dr}} = -6\pi\eta a\mathbf{v}$ , where  $\eta$  is the viscosity of the fluid. We will simplify the problem by assuming that the particles are made of a material which is much denser than the fluid in which they are suspended: this enables us to neglect the inertia of the displaced fluid. Accordingly, we consider a large number of suspended particles, initially with random positions and zero velocity, having equations of motion

$$\dot{\mathbf{r}} = \frac{1}{m}\mathbf{p}, \quad \dot{\mathbf{p}} = -\gamma[\mathbf{p} - m\mathbf{u}(\mathbf{r}, t)]. \quad (1)$$

The random velocity field  $\mathbf{u}(\mathbf{r}, t)$  could be either externally imposed (for example, if a gas is driven by an ultrasonic noise source), or self-generated (as in the case of turbulence). The equations of motion with displaced mass effects included are discussed in Ref. [18]. Our neglect of displaced mass effects is justified for aerosol systems. In order to fully specify the problem we must define the statistical properties of the random velocity field  $\mathbf{u}(\mathbf{r}, t)$ . The random force  $\mathbf{f} = m\gamma\mathbf{u}$  is generated from a vector potential  $\mathbf{A} = (A_1, A_2, A_3)$  and a scalar potential  $\phi = A_0$ :

$$\mathbf{f} = \nabla\phi + \nabla \wedge \mathbf{A}. \quad (2)$$

The scalar fields  $A_i(\mathbf{r}, t)$  have isotropic, homogeneous, and stationary statistics. We assume that these fields are statistically independent, and that they all have the same correlation function, except that the intensity of  $\phi = A_0$  exceeds that of the other fields by a factor  $1/\alpha^2$ :

$$\langle A_i(\mathbf{r}, t) A_j(\mathbf{r}', t') \rangle = \delta_{ij} [(1 - \alpha^2) \delta_{i0} + \alpha^2] C \left( \frac{|\mathbf{r} - \mathbf{r}'|}{\xi}, \frac{t - t'}{\tau} \right). \quad (3)$$

The random force  $\mathbf{f}(\mathbf{r}, t)$  is characterized by typical magnitude  $\sigma$ , correlation length  $\xi$ , and correlation time  $\tau$ . In the case of a well-developed turbulent flow, the velocity field has a power-law spectrum with upper and lower cutoffs [19]. If a random velocity field modeling fully developed turbulence is used in our model, it is most appropriate to take the correlation length and time to be those of the dissipation scale, that is, the cutoff with the smaller length scale.

The system of equations is characterized by three independent dimensionless parameters, which we take as

$$\nu = \gamma\tau, \quad \chi = \frac{\sigma\tau^2}{m\xi}, \quad \alpha. \quad (4)$$

The parameter  $\nu$  is a dimensionless measure of the degree of damping,  $\chi$  is a dimensionless measure of the strength of the forcing term, and  $\alpha$  determines the relative magnitudes of potential and solenoidal components of the velocity field (which is purely potential when  $\alpha=0$ , and purely solenoidal in the limit as  $\alpha \rightarrow \infty$ ). Later, immediately below Eq. (35), we will find it convenient to introduce an alternative measure of the relative strengths of potential and solenoidal components:  $\Gamma = (1 + 4\alpha^2)/(3 + 2\alpha^2)$ .

### C. Description of results

We show that the phase transition is determined by a Lyapunov exponent,  $\lambda_1$ , describing the separation of nearby particles: their trajectories coalesce if  $\lambda_1 < 0$ . Here we describe a general approach to this problem, reducing the determination of the Lyapunov exponent to the analysis of a simple dynamical system, described by a system of ordinary differential equations containing stochastic forcing terms: the Lyapunov exponent is found to be proportional to the expectation value of one coordinate. These stochastic differential equations are derived in Sec. II. They introduce an apparent paradox: the structure of the equations appears to be identical in two-dimensional and three-dimensional flows, suggesting that the path-coalescence transition is fundamentally the same in two and three dimensions. That would be a very surprising conclusion.

In order to demonstrate and illuminate our method, in Secs. III and IV we pursue the solution of this problem in considerable depth in one limiting case, namely the limit where the correlation time  $\tau$  of the random velocity field is small and the random force is sufficiently weak (strictly, we consider the case where  $\chi \ll \nu \ll 1$ ). In this limit, the system of ordinary differential equations described in Sec. II becomes a system of two coupled Langevin equations. In Sec. III we show that there is in fact a difference between the three-dimensional problem and the two-dimensional case studied in Ref. [12], which is a rather subtle example of the difficulties in applying Langevin approaches to nonlinear equations [20].

In Sec. IV we discuss a perturbation theory for the Lyapunov exponent describing the phase transition, ex-

panded in powers of a parameter  $\epsilon \sim \chi\nu^{-3/2}$  which is a dimensionless measure of the inertia of the particles. The perturbation theory is constructed by transforming the Langevin equation first into a Fokker-Planck equation, and then into a non-Hermitean perturbation of a three-dimensional isotropic quantum harmonic oscillator. We are then able to use the harmonic-oscillator creation and annihilation operators [21] to express the perturbation theory in a purely algebraic form, enabling us to compute the coefficients to any desired order. We investigate the phase diagram (the line in parameter space separating coalescing and noncoalescing phases), using both Monte Carlo averaging of the Langevin equation and the results of our perturbation theory. We find that aggregation can only occur if the random flow has a certain degree of compressibility, which increases as the effects of inertia increase, until there is no coalescing phase even for a purely potential flow field.

The analysis in Secs. II–IV considers the case where all of the suspended particles have the same mass  $m$  and damping rate  $\gamma$ . This ideal can be approached quite accurately in model experiments, but in most applications in the natural world and in technology, the suspended particles will have different masses, sizes, and shapes. In Sec. IV we discuss the effect of dispersion in the distribution of masses in the one-dimensional case: these arguments can be adapted to treat higher dimensions and dispersion of the damping constant  $\gamma$ . We argue that path coalescence is not destroyed by mass dispersion (although of course it is no longer a sharp transition).

In this paper we give a quite comprehensive discussion of the the case where the correlation time of the random flow is very short, and the stochastic differential equations derived in Sec. II can be approximated by Langevin equations. Section VI discusses how our approach can be extended to other cases.

## II. EQUATIONS DETERMINING THE LYAPUNOV EXPONENT

To determine whether particles cluster together, we consider two nearby trajectories with spatial separation  $\delta\mathbf{r}$  and momenta differing by  $\delta\mathbf{p}$ . The linearized equations of motion derived from (1) are

$$\delta\dot{\mathbf{r}} = \frac{1}{m} \delta\mathbf{p}, \quad \delta\dot{\mathbf{p}} = -\gamma\delta\mathbf{p} + \mathbf{F}(t) \delta\mathbf{r}. \quad (5)$$

Here  $\mathbf{F}(t)$  is proportional to the strain-rate matrix of the velocity field, with elements

$$F_{ij}(t) = \frac{\partial f_i}{\partial r_j}(\mathbf{r}(t), t) = m\gamma \frac{\partial u_i}{\partial r_j}(\mathbf{r}(t), t). \quad (6)$$

It is convenient to parametrize  $\delta\mathbf{r}$  and  $\delta\mathbf{p}$  as follows:

$$\delta\mathbf{r} = X\mathbf{n}_1, \quad \delta\mathbf{p} = X(Y_1\mathbf{n}_1 + Y_2\mathbf{n}_2), \quad (7)$$

where  $\mathbf{n}_1$  and  $\mathbf{n}_2$  are orthogonal unit vectors, which depend upon time. The parameter  $X$  is a scale factor: trajectories coalesce if  $X$  decreases with probability unity in the long-time limit. In the three-dimensional case, we find it conve-

nient to introduce the third element  $\mathbf{n}_3 = \mathbf{n}_1 \wedge \mathbf{n}_2$  of a time-dependent orthonormal basis so that

$$\mathbf{n}_i \cdot \mathbf{n}_j = \delta_{ij} \quad \text{and} \quad \mathbf{n}_i = \varepsilon_{ijk} \mathbf{n}_j \wedge \mathbf{n}_k. \quad (8)$$

Differentiating (7), and substituting the resulting expressions into (5) gives

$$\delta \dot{\mathbf{r}} = \dot{X} \mathbf{n}_1 + X \dot{\mathbf{n}}_1 = \frac{1}{m} X (Y_1 \mathbf{n}_1 + Y_2 \mathbf{n}_2),$$

$$\begin{aligned} \delta \dot{\mathbf{p}} &= \dot{X} (Y_1 \mathbf{n}_1 + Y_2 \mathbf{n}_2) + X (\dot{Y}_1 \mathbf{n}_1 + \dot{Y}_2 \mathbf{n}_2) + X (Y_1 \dot{\mathbf{n}}_1 + Y_2 \dot{\mathbf{n}}_2) \\ &= -\gamma X (Y_1 \mathbf{n}_1 + Y_2 \mathbf{n}_2) + \mathbf{F}(t) \mathbf{n}_1. \end{aligned} \quad (9)$$

Projecting  $\delta \dot{\mathbf{r}}$  onto the unit vectors  $\mathbf{n}_i$  gives the following three scalar equations of motion:

$$\mathbf{n}_1 \cdot \delta \dot{\mathbf{r}} = \dot{X} = \frac{1}{m} Y_1 X,$$

$$\mathbf{n}_2 \cdot \delta \dot{\mathbf{r}} = X (\mathbf{n}_2 \cdot \dot{\mathbf{n}}_1) = \frac{1}{m} Y_2 X, \quad (10)$$

$$\mathbf{n}_3 \cdot \delta \dot{\mathbf{r}} = X \dot{\mathbf{n}}_1 \cdot \mathbf{n}_3 = 0.$$

The last of these equations implies that  $\dot{\mathbf{n}}_1 \wedge \mathbf{n}_2 = \mathbf{0}$ , so that  $\dot{\mathbf{n}}_1$  is proportional to  $\mathbf{n}_2$ : we write

$$\dot{\mathbf{n}}_1 = \dot{\theta} \mathbf{n}_2 \quad (11)$$

so that the equation for  $\mathbf{n}_2 \cdot \delta \dot{\mathbf{r}}$  gives

$$\dot{\theta} = \frac{1}{m} Y_2. \quad (12)$$

The first equation of (10) indicates that  $X$  is a product of random variables, and therefore has a log-normal distribution, that is, the logarithm of  $X$  has a Gaussian probability density. In the limit as  $t \rightarrow \infty$ , the mean and variance of  $\log_e X$  are both linear functions of time:

$$\langle \log_e X \rangle \sim \lambda_1 t + c_1, \quad \text{var}(\log_e X) \sim \mu t + c_2, \quad (13)$$

where  $\lambda_1$ ,  $\mu$ ,  $c_1$ , and  $c_2$  are constants. If  $\lambda_1 < 0$ , the probability of  $\log_e X$  exceeding any specified value approaches zero as  $t \rightarrow \infty$ , implying that trajectories of nearby particles almost always coalesce.

The Lyapunov exponent  $\lambda_1$  is the mean value of the derivative  $d \log_e X / dt$ , so that the first equation of (10) gives

$$\lambda_1 = \frac{1}{m} \langle Y_1 \rangle. \quad (14)$$

Now consider the three projections of  $\delta \dot{\mathbf{p}}$ , as given by Eq. (9):

$$\mathbf{n}_1 \cdot \delta \dot{\mathbf{p}} = \dot{X} Y_1 + X \dot{Y}_1 + X Y_2 (\mathbf{n}_1 \cdot \dot{\mathbf{n}}_2) = -\gamma X Y_1 + \mathbf{n}_1 \cdot \mathbf{F}(t) \mathbf{n}_1 X,$$

$$\mathbf{n}_2 \cdot \delta \dot{\mathbf{p}} = \dot{X} Y_2 + X \dot{Y}_2 + X Y_1 (\dot{\mathbf{n}}_1 \cdot \mathbf{n}_2) = -\gamma X Y_2 + \mathbf{n}_2 \cdot \mathbf{F}(t) \mathbf{n}_1 X, \quad (15)$$

$$\mathbf{n}_3 \cdot \delta \dot{\mathbf{p}} = X Y_1 (\mathbf{n}_3 \cdot \dot{\mathbf{n}}_1) + X Y_2 (\mathbf{n}_3 \cdot \dot{\mathbf{n}}_2) = \mathbf{n}_3 \cdot \mathbf{F}(t) \mathbf{n}_1 X.$$

We introduce the notation

$$\mathbf{n}_i(t) \cdot \mathbf{F}(t) \mathbf{n}_j(t) = F'_{ij}(t) \quad (16)$$

and use Eqs. (10)–(12) and  $(\mathbf{n}_i \cdot \dot{\mathbf{n}}_j) + (\dot{\mathbf{n}}_i \cdot \mathbf{n}_j) = 0$  to simplify. We find the following equations of motion for the variables  $Y_i$ :

$$\dot{Y}_1 = -\gamma Y_1 + \frac{1}{m} (Y_2^2 - Y_1^2) + F'_{11}(t),$$

$$\dot{Y}_2 = -\gamma Y_2 - \frac{2}{m} Y_1 Y_2 + F'_{21}(t). \quad (17)$$

Finally, the equation for  $\mathbf{n}_3 \cdot \delta \dot{\mathbf{p}}$  gives

$$\mathbf{n}_2 \cdot \dot{\mathbf{n}}_3 = -\frac{1}{Y_2} F'_{31}(t). \quad (18)$$

Equations (14) and (17) are the principal results of this paper. Equation (14) shows that the Lyapunov exponent (the sign of which determines whether or not path coalescence occurs) is given by the expectation value of a random variable  $Y_1$  of a simple, finite dimensional stochastic dynamical system, described by Eqs. (17). This dynamical system is almost completely decoupled from the other variables: the equations for  $Y_1$  and  $Y_2$  do not depend upon  $X$ , and the vectors  $\mathbf{n}_i(t)$  only enter these equations through the evaluation of the random matrix elements  $F'_{ij}$ .

In the two-dimensional case the analysis leading to (17) proceeds along similar lines, and leads to the same pair of equations [12]. The only difference is that the equation (18) is absent in the two-dimensional case. This suggests that the expression for the Lyapunov exponent  $\lambda_1 = \langle Y_1 \rangle / m$  should be the same in two and three dimensions. This would be a surprising conclusion, but it is not obvious how it can be averted. However, it does prove to be false, as will be demonstrated in the next section for the limiting case where  $\chi \ll \nu \ll 1$ .

### III. THE LANGEVIN APPROXIMATION

Let us now consider how to treat Eqs. (17) in the limit where the correlation time  $\tau$  of  $\mathbf{F}(t)$  is very short. Because the random field  $\mathbf{f}(\mathbf{r}, t)$  is fluctuating very rapidly, the position  $\mathbf{r}(t)$  of a particle at time  $t$  is independent of the instantaneous value of the force  $\mathbf{f}(\mathbf{r}, t)$ , so that the value of  $F'_{ij}(t) = \partial f_i / \partial r_j(\mathbf{r}(t), t)$  at the position of the particle is statistically indistinguishable from a random sample of the field  $\partial f_i / \partial r_j$ . We also assume that the gradients of the fluctuating forces [the quantities  $F'_{11}$  and  $F'_{22}$  in Eqs. (17)] are sufficiently small that the typical magnitude of the displacement of the variables  $Y_1, Y_2$  occurring during the correlation time  $\tau$  is small compared to the typical magnitude of these variables. This condition is expressed in terms of the dimensionless variables  $\chi$  and  $\nu$  later in this section. Under these conditions of short correlation time and small amplitude, Eqs. (17) may be replaced by Langevin equations. At first sight, this would appear to lead to

$$dY_1 = \left( -\gamma Y_1 + \frac{1}{m}(Y_2^2 - Y_1^2) \right) dt + df_1,$$

$$dY_2 = \left( -\gamma Y_2 - \frac{2}{m} Y_1 Y_2 \right) dt + df_2, \quad (19)$$

where the  $df_i$  are increments of a Brownian process, satisfying  $\langle df_i \rangle = 0$  and  $\langle df_i df_j \rangle = 2D_{ij} dt$ , for some constant diffusion coefficients  $D_{ij}$ . In the two-dimensional case, this expectation is correct [12], and Eqs. (19) are the appropriate Langevin equations. In the three-dimensional case, we will see that an additional drift term must be added to the second of these equations. This is a consequence of the fact that, in the three-dimensional case,  $Y_2$  is a nonlinear function of the components of the vector  $\delta \mathbf{p} - Y_1 \delta \mathbf{r}$  because it is proportional to the magnitude of this vector. This is an example of the difficulties that arise when treating Langevin equations involving nonlinear functions of noise terms [20].

In order to determine the correct Langevin equations to model (17), let us consider the integral of the stochastic forcing terms over a time interval  $\delta t$  which is long compared to  $\tau$ , but short enough that the change in the variables  $Y_i$  occurring in time  $\delta t$  can be neglected. We define

$$\delta f_i(t) = \int_t^{t+\delta t} dt' F'_{i1}(t'), \quad (20)$$

and find

$$\langle \delta f_i \delta f_j \rangle = 2D_{ij} \delta t + O(\tau), \quad (21)$$

where

$$D_{ij} = \frac{1}{2} \int_{-\infty}^{\infty} dt \langle F'_{i1}(t) F'_{j1}(0) \rangle. \quad (22)$$

The calculation of  $\langle \delta f_i(t) \rangle$  is more subtle. We have

$$\langle \delta f_i \rangle = \int_0^{\delta t} dt \langle \mathbf{n}_i(t) \cdot \mathbf{F}(t) \mathbf{n}_1(t) \rangle. \quad (23)$$

We must take account of the fact that the unit vectors  $\mathbf{n}_i(t)$  are rotating: we write

$$\mathbf{n}_i(t) = \sum_{k=1}^3 R_{ik}(t) \mathbf{n}_k(0), \quad (24)$$

where  $R_{ik}(t)$  are elements of a rotation matrix. We now write (23) in the form

$$\langle \delta f_i \rangle = \int_0^{\delta t} dt \sum_{k=1}^3 \sum_{l=1}^3 \langle R_{ik}(t) R_{1l}(t) F'_{kl}(t) \rangle. \quad (25)$$

Now consider the rotation of the unit vectors: using (14) and (18) we have

$$\mathbf{n}_1(t) = \mathbf{n}_1(0) + \dot{\theta} \mathbf{n}_2(0)t + O(t^2),$$

$$\mathbf{n}_2(t) = \mathbf{n}_2(0) - \dot{\theta} \mathbf{n}_1(0)t + \frac{1}{Y_2} \int_0^t dt' F'_{31}(t') \mathbf{n}_3(0) + O(t^2), \quad (26)$$

$$\mathbf{n}_3(t) = \mathbf{n}_3(0) - \frac{1}{Y_2} \int_0^t dt' F'_{31}(t') \mathbf{n}_2(0) + O(t^2),$$

so that

$$\mathbf{R}(t) = \begin{pmatrix} 1 & \dot{\theta} t & 0 \\ -\dot{\theta} t & 1 & Y_2^{-1} \int_0^t dt' F'_{31} \\ 0 & -Y_2^{-1} \int_0^t dt' F'_{31} & 1 \end{pmatrix} + O(t^2). \quad (27)$$

We obtain

$$\begin{aligned} \langle \delta f_i \rangle &= \int_0^{\delta t} dt \sum_k \langle R_{ik}(t) F'_{k1}(t) + \dot{\theta} t F'_{k2}(t) \rangle + O(\delta t^2) \\ &= \int_0^{\delta t} dt \sum_k \langle R_{ik}(t) F'_{k1}(t) \rangle + O(\delta t^2). \end{aligned} \quad (28)$$

This yields

$$\begin{aligned} \lim_{\delta t \rightarrow 0} \frac{1}{\delta t} \langle \delta f_1 \rangle &= \frac{1}{\delta t} \int_0^{\delta t} dt \langle F'_{11}(t) + \dot{\theta} t F'_{21}(t) \rangle = 0, \\ \lim_{\delta t \rightarrow 0} \frac{1}{\delta t} \langle \delta f_2 \rangle &= \frac{1}{\delta t} \int_0^{\delta t} dt \left\langle -\dot{\theta} t F'_{11}(t) + F'_{21}(t) \right. \\ &\quad \left. + \frac{1}{Y_2} \int_0^t dt' F'_{31}(t) F'_{31}(t') \right\rangle \\ &= \frac{1}{Y_2 \delta t} \int_0^{\delta t} dt \int_0^t dt' \langle F'_{31}(t) F'_{31}(t') \rangle = \frac{1}{Y_2} D_{31}. \end{aligned} \quad (29)$$

The Langevin equations therefore contain an additional drift term due to the fact that  $\langle \delta f_2 \rangle$  is nonzero: the correct Langevin equations in three dimensions are

$$dY_1 = \left( -\gamma Y_1 + \frac{1}{m}(Y_2^2 - Y_1^2) \right) dt + d\zeta_1,$$

$$dY_2 = \left( -\gamma Y_2 + \frac{D_{31}}{Y_2} - \frac{2}{m} Y_1 Y_2 \right) dt + d\zeta_2, \quad (30)$$

with

$$\langle d\zeta_i \rangle = 0, \quad \langle d\zeta_i d\zeta_j \rangle = 2D_{ij} dt. \quad (31)$$

The diffusion constants  $D_{ij}$  were defined in Eq. (22). Note that in two dimensions, however, (19) remains valid because the term arising from the rotation of  $\mathbf{n}_3$  is absent [12].

Now consider the evaluation of the diffusion constants in terms of the statistics of the force  $\mathbf{f}(\mathbf{r}, t)$ . The statistics of the transformed matrix elements  $F'_{ij}(t)$  are the same as those of the original elements  $F_{ij}(t)$ , because the statistics of the velocity field are isotropic. The elements of the force-gradient matrix  $\mathbf{F}$  are

$$F_{ij} = \frac{\partial^2 \phi}{\partial r_i \partial r_j} + \sum_{k=1}^3 \sum_{l=1}^3 \epsilon_{ilk} \frac{\partial^2 A_k}{\partial r_j \partial r_l}, \quad (32)$$

where  $\epsilon_{ilk}$  is the ‘‘Kronecker  $\epsilon$ -symbol’’ describing the parity of the permutation of the indices  $ilk$ . We define

$$D_0 = \frac{1}{2} \int_{-\infty}^{\infty} dt \left\langle \frac{\partial^2 \phi}{\partial r_1^2}(t) \frac{\partial^2 \phi}{\partial r_1^2}(0) \right\rangle \quad (33)$$

and  $D_1 = D_{11}$ ,  $D_2 = D_{21} = D_{31}$ , so that

$$D_1 = D_0 \left( 1 + \frac{2\alpha^2}{3} \right) \quad \text{and} \quad D_2 = D_0 \left( \frac{1}{3} + \frac{4\alpha^2}{3} \right). \quad (34)$$

We introduce a more convenient dimensionless measure of the relative importance of solenoidal and potential fields as in Ref. [12],

$$\Gamma \equiv \frac{D_2}{D_1}. \quad (35)$$

From (34) we find that  $\Gamma = (1 + 4\alpha^2)/(3 + 2\alpha^2)$ , so that  $\frac{1}{3} \leq \Gamma \leq 2$  (since  $0 \leq \alpha \leq \infty$ ):  $\Gamma = \frac{1}{3}$  corresponds to purely potential flow, while  $\Gamma = 2$  corresponds to purely solenoidal flow. In two dimensions, by contrast, we found  $\Gamma = (1 + 3\alpha^2)/(3 + \alpha^2)$ , so that  $\frac{1}{3} \leq \Gamma \leq 3$  [12].

It is convenient to rescale the Langevin equations into dimensionless form. We write

$$dt' = \gamma dt, \quad x_i = \sqrt{\frac{\gamma}{D_i}} Y_i, \quad dw_i = \sqrt{\frac{\gamma}{D_i}} d\zeta_i \quad (36)$$

and define

$$\epsilon = \frac{D_1^{1/2}}{m \gamma^{3/2}}. \quad (37)$$

The dimensionless parameter  $\epsilon$  is related to those defined in Eq. (4):  $\epsilon \sim \chi \nu^{-3/2}$ . With these changes of variables, the Langevin equations become

$$\begin{aligned} dx_1 &= [-x_1 + \epsilon(\Gamma x_2^2 - x_1^2)] dt' + dw_1, \\ dx_2 &= [-x_2 + x_2^{-1} - 2\epsilon x_1 x_2] dt' + dw_2, \end{aligned} \quad (38)$$

with

$$\langle dw_i \rangle = 0, \quad \langle dw_i dw_j \rangle = 2 \delta_{ij} dt'. \quad (39)$$

Equations (38) must be solved to determine the expectation value of  $x_1$  in the steady state. The Lyapunov exponent is then given by

$$\lambda_1 = \gamma \epsilon \langle x_1 \rangle. \quad (40)$$

Figure 2(a) compares the Lyapunov exponent obtained from a Monte Carlo simulation of Eqs. (38)–(40) with a direct numerical simulation of a random flow described by Eq. (1). The Lyapunov exponents determined from Eqs. (38) and (39) for  $\Gamma = 1/3, 1$ , and  $2$  are plotted as solid (red) lines. The results are compared to numerical simulations of (1), using a method described in Ref. [15] to determine the Lyapunov exponent. Because we are concerned with the limit where the

correlation time  $\tau$  is taken to zero, the random flow was generated using a discrete series of uncorrelated random impulses, acting over a small time step  $\delta t \gg \tau$ : the impulse

$$\mathbf{f}_n(\mathbf{r}) = \int_{n\delta t}^{(n+1)\delta t} dt' \mathbf{f}(\mathbf{r}', t') \quad (41)$$

at time  $n \delta t$  is taken to be of the form (2) in terms of scalar fields  $\phi_n(\mathbf{r})$  and  $\mathbf{A}_n(\mathbf{r})$  satisfying

$$\langle \phi_n(\mathbf{r}) \phi_{n'}(\mathbf{r}') \rangle = \sigma^2 \xi^2 \delta t \exp(-|\mathbf{r} - \mathbf{r}'|^2 / 2\xi^2) \delta_{nn'}, \quad (42)$$

and similarly for  $\mathbf{A}_n(\mathbf{r})$ . This implies

$$D_0 = 3\sigma^2 / (2m^2 \gamma^3 \xi^2). \quad (43)$$

Now we discuss the conditions under which the Langevin equations (38) and (39) are a valid approximation of (17) and (18). For this purpose it is sufficient to consider the one-dimensional version of Eqs. (30), namely

$$\dot{Y} = -\gamma Y - \frac{1}{m} Y^2 + F(t) \quad (44)$$

(this equation appears with a different notation in Ref. [13]). The Langevin equations are valid provided the changes in the value of  $Y$  over the correlation time  $\tau$  is small compared to the typical values of this quantity. This criterion can obviously only be satisfied if the correlation time is sufficiently short that  $\nu = \gamma\tau \ll 1$ . The criterion also requires the stochastic force  $F(t)$  to be sufficiently weak. The deterministic part of the velocity,  $-\gamma Y - Y^2/m$ , is positive in the interval from  $Y = -\gamma m$  to  $Y = 0$ . The criterion on the strength of  $F \sim \sigma/\xi$  is that the displacement over time  $\tau$  should be small compared to the width of that interval, that is  $|F|\tau \ll \gamma m$ . Using the fact that  $|F| \sim \sigma/\xi$ , we obtain the following criteria for the validity of the Langevin approximation:

$$\frac{\chi}{\nu} \ll 1, \quad \nu \ll 1. \quad (45)$$

#### IV. PERTURBATION THEORY

We now show how to obtain an asymptotic approximation for the Lyapunov exponent using Eqs. (38) and (39). These equations are equivalent to a two-dimensional Fokker-Planck equation (Ref. [20]) for a probability density  $P(x_1, x_2; t')$ , of the form

$$\partial_{t'} P = D \Delta P - \nabla \cdot (\mathbf{v} P) = \hat{\mathcal{F}} P. \quad (46)$$

Here the diffusion constant  $D = 1$  and the drift velocity is  $\mathbf{v} = (v_1, v_2)$  with components  $v_1 = -x_1 + \epsilon(\Gamma x_2^2 - x_1^2)$  and  $v_2 = -x_2 + x_2^{-1} - 2\epsilon x_1 x_2$ . We write  $\hat{\mathcal{F}} = \hat{\mathcal{F}}_0 + \epsilon \hat{\mathcal{F}}_1$ , and seek a steady-state solution satisfying  $\hat{\mathcal{F}} P = 0$  by perturbation theory in  $\epsilon$ . In order to simplify the application of perturbation theory, it is convenient to make a transformation so that the unperturbed Fokker-Planck operator  $\hat{\mathcal{F}}_0$  is transformed into a Hermitian operator. Rather than proceeding to the Hermitian form directly, we first map the two-dimensional Fokker-Planck

equation to a three-dimensional equation with a rotational symmetry (we seek a solution which is invariant under rotation). After making this transformation, we find that the corresponding Hermitian operator in three-dimensional space is the Schrödinger operator of an isotropic three-dimensional harmonic oscillator. The perturbation analysis can then be performed very easily, using the algebra of harmonic-oscillator raising and lowering operators, described in Ref. [21]. To shorten equations, we will use a variant of the Dirac notation scheme: in summary, functions  $a$ ,  $b$  are symbolized by vectors  $|a\rangle$ ,  $|b\rangle$ , linear operators are denoted by a hat, e.g.,  $\hat{A}$ , and the integral over all space of the product of two functions is denoted by the inner product  $(a|b)$ .

In the original form, the action of the unperturbed part of the Fokker-Planck operator on a function  $P$  is

$$\hat{\mathcal{F}}_0 P = (\partial_1^2 + \partial_2^2)P + \partial_1(x_1 P) + \partial_2[(x_2 - x_2^{-1})P]. \quad (47)$$

We transform this by defining the action of  $\hat{\mathcal{F}}'_0$  on a function  $P' = P/x_2$  as follows:

$$\begin{aligned} \hat{\mathcal{F}}'_0 P' &= \frac{1}{x_2} \hat{\mathcal{F}}_0 P \\ &= \frac{1}{x_2} (\partial_1^2 + \partial_2^2)(x_2 P') + \frac{1}{x_2} \partial_1(x_1 x_2 P') + \frac{1}{x_2} \partial_2[(x_2^2 - 1)P'] \\ &= \partial_1[(\partial_1 + x_1)P'] + \frac{1}{x_2} \partial_2[x_2(\partial_2 + x_2)P']. \end{aligned} \quad (48)$$

We now consider  $\hat{\mathcal{F}}'_0$  to be an operator acting in three-dimensional space, with cylindrical polar coordinates  $(r, \varphi, z)$ . We identify  $r=x_2$ , and  $z=x_1$ , and take  $P'$  to be a function which is restricted so that it has cylindrical symmetry, being independent of  $\varphi$ . With this interpretation, we can add differentials with respect to  $\phi$  to the definition of  $\hat{\mathcal{F}}'_0$ , and write

$$\hat{\mathcal{F}}'_0 = \frac{1}{r} \partial_r[r(\partial_r + r)] + \frac{1}{r^2} \partial_\varphi^2 + \partial_z(\partial_z + z) \quad (49)$$

which is the Fokker-Planck operator for isotropic diffusion in three-dimensional space (with  $D=1$ ). Thus we have transformed the two-dimensional Fokker-Planck equation to a three-dimensional one with a very simple unperturbed velocity field. It is convenient to work with Cartesian coordinates  $\mathbf{x}=(x, y, z)$  in the three-dimensional space, having the usual relation to the cylindrical polar coordinates  $(r, \varphi, z)$ . The Fokker-Planck equation is then

$$\partial_t P' = \nabla^2 P' + \nabla \cdot [(\mathbf{x} - \epsilon \mathbf{v}'_1)P'] = \hat{\mathcal{F}}' P' = [\hat{\mathcal{F}}'_0 + \epsilon \hat{\mathcal{F}}'_1] P', \quad (50)$$

where, in Cartesian coordinates,  $\mathbf{v}'_1$  is (expressed as a row vector):

$$\mathbf{v}'_1 = (-2xz, -2yz, -z^2 + \Gamma(x^2 + y^2)). \quad (51)$$

We now transform the Fokker-Planck operator  $\hat{\mathcal{F}}'$  so that  $\hat{\mathcal{F}}'_0$  turns into a very simple Hermitian operator, by writing

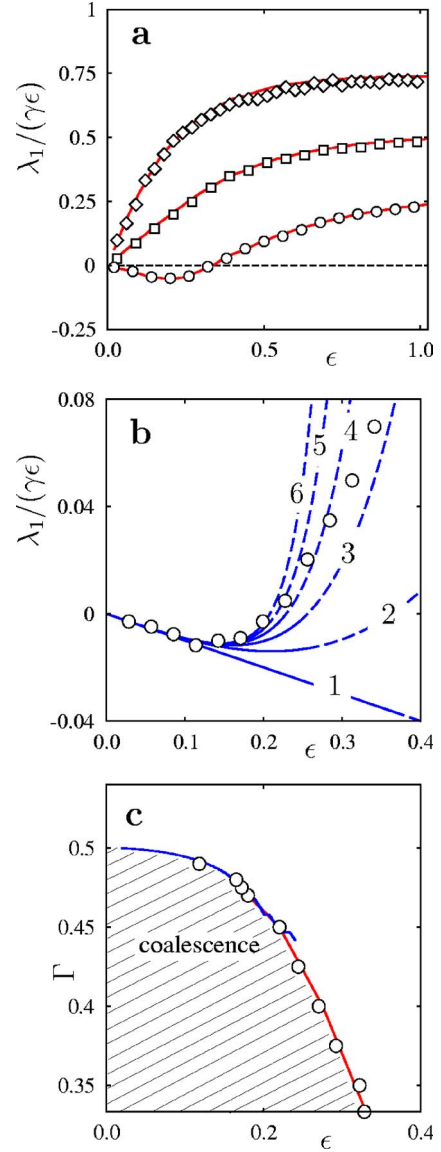


FIG. 2. (Color online) (a) Lyapunov exponent as a function of  $\epsilon$ , for a small value of  $\chi$ , results from Eqs. (38), (39), and (40) are shown as solid lines, those from direct simulations as symbols,  $\Gamma = 1/3$  ( $\circ$ ),  $\Gamma = 1$  ( $\square$ ), and  $\Gamma = 2$  ( $\diamond$ ). The simulations were performed with a simplified version of the dynamics using Eqs. (41) and (42). (b) Lyapunov exponent  $\lambda_1/(\epsilon\gamma)$  versus  $\epsilon$  for  $\Gamma = 0.45$ . Shown are results from simulations ( $\circ$ ) as well as from the asymptotic series (68) summed to orders  $l_{\max} = 1, \dots, 6$ : up to  $\epsilon^*(l_{\max})$  full lines and from  $\epsilon^*(l_{\max})$  dashed lines. The simulations were performed by replacing the components of  $\mathbf{f}_r(\mathbf{r})$  in (41) by random numbers with the appropriate distributions. (c) Phase diagram in the  $\epsilon$ - $\Gamma$  plane. Shown are results from numerical simulations as described above,  $\circ$ , summation of the asymptotic series (68) summed to  $l_{\max}^*(\epsilon)$ , [(blue) line, showing discontinuities where  $l_{\max}^*$  changes and plotted for  $\epsilon < 0.25$ ], as well as results from Langevin simulations [smooth (red) line].

$$\hat{\mathcal{H}} = \exp(\Phi_0/2) \hat{\mathcal{F}}' \exp(-\Phi_0/2) \quad (52)$$

with  $\Phi_0 = \frac{1}{2}(x^2 + y^2 + z^2)$ . We find

$$\hat{\mathcal{H}}_0 = \exp(\Phi_0/2)\hat{\mathcal{F}}_0' \exp(-\Phi_0/2) = \nabla^2 + \frac{1}{4}(x^2 + y^2 + z^2) + \frac{3}{2} \quad (53)$$

so that  $\hat{\mathcal{H}}_0$  is (apart from a negative multiplicative factor) the Hamiltonian operator for a three-dimensional harmonic oscillator. The spectrum of  $\hat{\mathcal{H}}_0$  is the set of nonpositive integers  $(0, -1, -2, -3, \dots)$ . The eigenfunctions of  $\hat{\mathcal{H}}_0$  are generated by raising and lowering operators [21],

$$\hat{a}_x = \frac{1}{2}x + \partial_x, \quad \hat{a}_x^+ = \frac{1}{2}x - \partial_x \quad (54)$$

and similarly for the  $y$  and  $z$  coordinates. The transformed perturbation operator is

$$\hat{\mathcal{H}}_1 = -2\hat{a}_x^+\hat{x}\hat{z} - 2\hat{a}_y^+\hat{y}\hat{z} - \hat{a}_z^+[z^2 - \Gamma(\hat{x}^2 + \hat{y}^2)]. \quad (55)$$

Instead of solving the Fokker-Planck equation  $\hat{\mathcal{F}}'P' = 0$  we attempt to solve  $\hat{\mathcal{H}}Q = 0$ , where  $Q = \exp(\Phi_0/2)P'$ .

Now consider how to obtain the Lyapunov exponent from the function  $Q$ . We have  $\lambda_1 = \gamma\epsilon\langle z \rangle$ . We calculate the average of  $z$  as follows:

$$\begin{aligned} \langle z \rangle &= \int_0^\infty dr \int_{-\infty}^\infty dz P(r, z) \\ &= \int_0^\infty r dr \int_0^{2\pi} d\varphi \int_{-\infty}^\infty dz z P'(r, z) \\ &= \int_{-\infty}^\infty dx \int_{-\infty}^\infty dy \int_{-\infty}^\infty dz z e^{-\Phi_0/2} Q(x, y, z). \end{aligned} \quad (56)$$

Now we change the notation, using a variant of the Dirac notation to represent the function  $Q$  by a ket vector  $|Q\rangle$ . Allowing for the possibility that  $|Q\rangle$  is not normalized, we write

$$\langle z \rangle = \frac{(\phi_{000}|\hat{z}_3|Q)}{(\phi_{000}|Q)} = \frac{(\phi_{000}|\hat{a}_3|Q)}{(\phi_{000}|Q)}, \quad (57)$$

where  $|\phi_{000}\rangle$  is the ground-state eigenfunction of  $\mathcal{H}_0$ , given by the function  $\exp(-\Phi_0/2) = \exp[-(x^2 + y^2 + z^2)/4]$ .

We calculate  $|Q\rangle$  by perturbation theory, writing

$$|Q\rangle = |Q_0\rangle + \epsilon|Q_1\rangle + \epsilon^2|Q_2\rangle + \dots \quad (58)$$

we find that the functions  $|Q_k\rangle$  satisfy the recursion relation

$$|Q_{k+1}\rangle = -\hat{\mathcal{H}}_0^{-1}\hat{\mathcal{H}}_1|Q_k\rangle. \quad (59)$$

At first sight this appears to be ill defined because one of the eigenvalues of  $\mathcal{H}_0$  is zero, so that the inverse of  $\mathcal{H}_0$  is only defined for the subspace of functions which are orthogonal to the ground state,  $|\phi_{000}\rangle$ . However, because all of the components of  $\mathcal{H}_1$  have a creation operator as a left factor, the function  $\hat{\mathcal{H}}_1|\psi\rangle$  is orthogonal to  $|\psi\rangle$  for any function  $|\psi\rangle$ , so that (59) is in fact well defined. The iteration starts with  $|Q_0\rangle = |\phi_{000}\rangle$ . The functions  $|Q_k\rangle$  should all have rotational symmetry about the  $z$  axis. The angular-momentum operator  $\hat{\mathcal{J}}_z = \hat{p}_x\hat{y} - \hat{p}_y\hat{x}$  commutes with both  $\hat{\mathcal{H}}_0$  and  $\hat{\mathcal{H}}_1$  (that is,  $[\hat{\mathcal{H}}_0, \hat{\mathcal{J}}_z] = 0$  and  $[\hat{\mathcal{H}}_1, \hat{\mathcal{J}}_z] = 0$  where we use square brackets

for the commutator,  $[\hat{A}, \hat{B}] = \hat{A}\hat{B} - \hat{B}\hat{A}$ ). The operators  $\hat{\mathcal{H}}_0$  and  $\hat{\mathcal{H}}_1$  can therefore be simultaneously reduced to block diagonal form, with blocks labelled by eigenvalues of  $\hat{\mathcal{J}}_z$ . We can restrict ourselves to the subspace where the eigenvalue of  $\hat{\mathcal{J}}_z$  is zero. The functions of this subspace are generated from the ground state using transformed raising and lowering operators, defined as follows:

$$\hat{\alpha}_+ = \frac{1}{\sqrt{2}}(\hat{a}_x + i\hat{a}_y), \quad \hat{\alpha}_- = \frac{1}{\sqrt{2}}(\hat{a}_x - i\hat{a}_y). \quad (60)$$

The transformed operators  $\hat{\alpha}_+$  and  $\hat{\alpha}_-$  satisfy  $[\hat{\alpha}_\pm, \hat{\alpha}_\pm^\dagger] = \hat{I}$  (where  $\hat{I}$  is the identity operator), which is the fundamental relation describing harmonic-oscillator raising and lowering operators. Expressing  $\hat{\mathcal{H}}_0$  and  $\hat{\mathcal{J}}_z$  in terms of these operators, we find

$$\hat{\mathcal{J}}_3 = \hat{\alpha}_-^\dagger\hat{\alpha}_- - \hat{\alpha}_+^\dagger\hat{\alpha}_+$$

$$\hat{\mathcal{H}}_0 = -(\hat{\alpha}_-^\dagger\hat{\alpha}_- + \hat{\alpha}_+^\dagger\hat{\alpha}_+ + a_z^\dagger a_z). \quad (61)$$

Using results from [21], we see that both  $\hat{\mathcal{H}}_0$  and  $\hat{\mathcal{J}}_z$  are linear combinations of harmonic-oscillator Hamiltonians,  $\hat{\alpha}_-^\dagger\hat{\alpha}_-$ ,  $\hat{\alpha}_+^\dagger\hat{\alpha}_+$ , and  $\hat{a}_z^\dagger\hat{a}_z$ . The  $n$ th eigenfunction  $|\phi_n\rangle$  of a harmonic-oscillator Hamiltonian  $\hat{a}^\dagger\hat{a}$  is obtained from its ground state  $|\phi_0\rangle$  by repeated application of the raising operator  $\hat{a}^\dagger$ :

$$|\phi_n\rangle = \frac{1}{\sqrt{n!}}(\hat{a}^\dagger)^n|\phi_0\rangle \quad (62)$$

and this eigenfunction has eigenvalue  $n$ . Thus eigenfunctions of  $\hat{\mathcal{H}}_0$  and  $\hat{\mathcal{J}}_z$  with zero angular momentum are constructed as follows:

$$|\psi_{nm}\rangle = \frac{1}{n!} \frac{1}{\sqrt{m!}} (\hat{\alpha}_-^\dagger)^n (\hat{\alpha}_+^\dagger)^m (\hat{a}_z^\dagger)^m |\phi_{000}\rangle \quad (63)$$

for  $n=0, 1, \dots$  and  $m=0, 1, \dots$ . The corresponding eigenvalues of  $\hat{\mathcal{H}}_0$  are  $-2n - m$ . The functions  $|Q_k\rangle$  are expanded in terms of the  $|\psi_{nm}\rangle$ , with coefficients  $a_{nm}^{(k)}$ :

$$|Q_k\rangle = \sum_{n=0}^{\infty} \sum_{m=0}^{\infty} a_{nm}^{(k)} |\psi_{nm}\rangle. \quad (64)$$

By projecting Eq. (59) onto the vector  $|\psi_{nm}\rangle$  and using the fact that the eigenvectors  $|\psi_{n'm'}\rangle$  of  $\hat{\mathcal{H}}_0$  form a complete basis, the iteration can be expressed as follows [for  $(n, m) \neq (0, 0)$ ]:

$$a_{nm}^{(k+1)} = \sum_{n'=0}^{\infty} \sum_{m'=0}^{\infty} \frac{(\psi_{nm}|\hat{\mathcal{H}}_1|\psi_{n'm'})}{2n+m} a_{n'm'}^{(k)}. \quad (65)$$

The matrix elements  $(\psi_{nm}|\hat{\mathcal{H}}_1|\psi_{n'm'})$  are readily computed using the algebraic properties of the raising and lowering operators, as discussed in Ref. [21]. The coefficients  $a_{nm}^{(k)}$  are then calculated recursively. This allows us to obtain the functions  $|Q_k\rangle$ . The lowest order is  $|Q_0\rangle = |\phi_{000}\rangle$ . Its contribution



to  $\lambda_1$  vanishes in view of (55). The leading order is

$$|Q_1\rangle = -\frac{4}{3}|\psi_{11}\rangle - |\psi_{01}\rangle - \frac{\sqrt{6}}{3}|\psi_{03}\rangle + 2\Gamma|\psi_{01}\rangle + \frac{2\Gamma}{3}|\psi_{11}\rangle. \quad (66)$$

The next order,  $|Q_2\rangle$ , does not contribute to  $\lambda_1$  since  $\hat{\mathcal{H}}_1|Q_1\rangle$  does not contain  $|\psi_{01}\rangle$ . In fact, only odd orders contain  $|\psi_{01}\rangle$  and thus give nonzero contributions to  $\lambda_1$ . We also find that the denominator in (58) is unity at all orders. The final result is:

$$\lambda_1 = \gamma\epsilon \sum_{l=1}^{\infty} c_l(\Gamma)\epsilon^{2l-1}, \quad (67)$$

where the first five coefficients  $c_l(\Gamma)$  are

$$c_1(\Gamma) = -1 + 2\Gamma,$$

$$c_2(\Gamma) = -5 + 20\Gamma - 16\Gamma^2,$$

$$c_3(\Gamma) = -60 + 360\Gamma - 568\Gamma^2 + 272\Gamma^3,$$

$$c_4(\Gamma) = -1105 + 8840\Gamma - 61936/3\Gamma^2 + 58432/3\Gamma^3 - 19648/3\Gamma^4,$$

$$c_5(\Gamma) = -27120 + 271200\Gamma - 7507040/9\Gamma^2 + 3492160/3\Gamma^3 - 2316032/3\Gamma^4 + 1785856/9\Gamma^5. \quad (68)$$

The coefficients  $c_l(\Gamma)$  increase rapidly, having a factorial times power growth as  $l \rightarrow \infty$  which is typical of asymptotic series [22]. Figure 2(b) shows approximations to the Lyapunov exponent  $\lambda_1$  for  $\Gamma=0.45$ . Shown are six different partial sums of the series (67), including terms up to  $l_{\max}$ , with  $l_{\max}=1, \dots, 6$ . For a given value of  $\epsilon$ , there is an optimal value of  $l_{\max}$ , which we term  $l_{\max}^*$ , defined by the criterion that the term in (67) with index  $l_{\max}^*$  is smallest in magnitude. The function  $l_{\max}^*(\epsilon)$  can be inverted, its inverse  $\epsilon^*(l_{\max})$  is the value of  $\epsilon$  for which the  $l_{\max}$  term is optimal. For values of  $\epsilon$  less than the  $\epsilon^*(l_{\max})$  the results are shown as solid lines. Beyond this value of  $\epsilon$ , the results are shown as dashed lines. The results show that, for sufficiently large  $l_{\max}$ , the series agrees well with the numerical simulation up to  $\epsilon^*$ , as would be expected for an asymptotic series.

The phase boundary in the  $\epsilon$ - $\Gamma$  plane is determined by the condition  $\lambda_1=0$ . Figure 2(c) shows this phase boundary as determined from truncating the series (68) at the optimal order  $l_{\max}^*(\epsilon)$  [(blue) line, showing discontinuities where  $l_{\max}^*$  changes]. This asymptotic result is shown for values of  $\epsilon$  up to  $\approx 0.25$ . Beyond this range, the asymptotic approximation becomes increasingly inaccurate. Also shown, in the same plot, are results obtained from the Langevin equations [Eqs. (38), (39), and (40)], and from direct simulations (○). The results show that the coalescing phase disappears as the effect of inertia is increased: the coalescing disappears altogether for the case of pure potential flow ( $\Gamma=\frac{1}{3}$ ) at  $\epsilon \approx 0.33$ .

One notable difference between the three-dimensional calculation presented here and the two-dimensional case considered in Ref. [12] is that in the two-dimensional case the phase boundary has a power series in  $\epsilon$  which vanishes identically.

## V. EFFECT OF DISPERSION OF PARTICLE MASSES

In most naturally occurring aerosols the suspended particles have different mass  $m$ , and particles of differing sizes will also have different values of the damping coefficient  $\gamma$ . It is important to consider whether particles still have a tendency to coalesce even when the particles have differing values of  $m$  and  $\gamma$ : we argue that the path coalescence effect is not destroyed by small mass dispersion. The argument can be adapted to dispersion of the damping coefficient, reaching the same conclusion.

Assume that the path-coalescence effect occurs for particles of mass  $m$ . Compare the motion of this reference particle with that of an initially nearby particle with mass  $m + \delta m$ . The reference particle has equation of motion

$$m\ddot{x} = -\gamma m\dot{x} + f(x, t). \quad (69)$$

Writing  $f(x + \delta x, t) = f(x, t) + F(t)\delta x + O(\delta x^2)$ , the equation of motion for the other particle is

$$(m + \delta m)(\ddot{x} + \delta\ddot{x}) = -\gamma m(\dot{x} + \delta\dot{x}) + f(x, t) + F(t)\delta x + O(\delta x^2). \quad (70)$$

Collecting the terms which are first order in  $\delta x$ , we obtain a linearized equation of motion for  $\delta x$ ,

$$-m\delta\ddot{x} - \gamma m\delta\dot{x} + F(t)\delta x = \delta m\ddot{x}. \quad (71)$$

This is an inhomogeneous differential equation for the separation  $\delta x$  between two particles, with a driving term proportional to their mass difference  $\delta m$ . The solution of this equation can be constructed from a Green's function satisfying  $G(t, t_0)$ ,

$$-m\frac{d^2G}{dt^2} - \gamma m\frac{dG}{dt} + F(t)G = \delta(t - t_0) \quad (72)$$

with  $G(t, t_0)=0$  for  $t < t_0$ . The solution of Eq. (71) is

$$\delta x(t) = \delta m \int_0^t dt' G(t, t') \frac{d^2x(t')}{dt'^2}. \quad (73)$$

For  $t > t_0$ , Eq. (72) is the equation for small displacements of trajectories of particles with the same mass. We know that in the path-coalescing phase the solutions have a negative value of the Lyapunov exponent  $\lambda_1$ , and that they therefore decay exponentially at large time. In the case where  $G(t, t')$  is bounded by an exponentially decreasing function, such that  $|G(t, t')| < A \exp(-\lambda_1|t - t'|)$ , Eq. (73) remains finite as  $t \rightarrow \infty$ . For sufficiently large  $A$ , the probability of this inequality being violated is extremely small. This indicates that in the path-coalescing phase the solution (73) remains finite as  $t \rightarrow \infty$ , except for very rare events. The conclusion is that, when  $\lambda_1 < 0$ , two initially close particles with nearly equal mass will remain in close proximity for a very long time.

## VI. DISCUSSION

In this paper we described the path-coalescence transition, and showed that the transition point is determined by the change of sign of a Lyapunov exponent. We showed that in general the Lyapunov exponent is determined from an expectation value of a variable of a simple dynamical system, Eqs. (17), which is driven by stochastic forcing functions. We considered the solution of these equations in a particular limiting case, where the dimensionless parameters satisfy  $\chi \ll \nu \ll 1$ , by mapping the continuous differential equations into a pair of coupled Langevin equations. We used these Langevin equations to produce a rather complete description of the phase transition in that limit. The remainder of these concluding remarks discuss how Eqs. (17) can be used in the case where these inequalities are not satisfied.

In order to solve these differential equations it is necessary to characterize the statistics of the stochastic driving terms  $F'_{ij}(t)$ . These terms contain information about the strain-rate of the field evaluated at a point along the reference particle trajectory. There are two possibilities:

Case A: The statistics of the strain-rate tensor along a trajectory may be indistinguishable from those sampled along a randomly chosen trajectory.

Case B: The trajectory may select regions where the strain-rate tensor has atypical properties, for example, by tracking points where the velocity vector  $\mathbf{u}$  vanishes.

If case A is realized there are two further possibilities:

Case A1: The trajectory  $\mathbf{r}(t)$  is sufficiently slowly moving that the displacement over time  $\tau$  is small compared to  $\xi$ . In this case the statistics of  $F'_{ij}$  are those of a randomly chosen static point, and the correlation time of  $F'_{ij}(t)$  will be  $\tau$ .

Case A2: If the trajectory  $\mathbf{r}(t)$  is moving sufficiently rapidly that its displacement in time  $\tau$  is large compared to  $\xi$ , then the correlation time of  $F'_{ij}(t)$  will be smaller than  $\tau$  because the loss of correlations results primarily from changing the position at which  $\partial u_i / \partial r_j(\mathbf{r}, t)$  is sampled.

The limit which was investigated in detail in this paper ( $\chi \ll \nu \ll 1$ ) is an example of case A1. In cases where  $\chi$  and  $\nu$  approach different limits however, all three possibilities can occur in the system described by Eqs. (1)–(3).

B.M. acknowledges financial support from Vetenskapsrådet.

- 
- [1] J. Sommerer and E. Ott, *Science* **359**, 334 (1993).  
 [2] J. R. Cressman, W. I. Goldberg, and J. Schuhmacher, *Europhys. Lett.* **66**, 219 (2004).  
 [3] J. R. Fessler, J. D. Kulick, and J. K. Eaton, *Phys. Fluids* **6**, 3742 (1994).  
 [4] B. van Haarlem, B. J. Boersma, and F. T. M Nieuwstadt, *Phys. Fluids* **10**, 2608 (1998).  
 [5] V. I. Klyatskin and D. Gurarie, *Phys. Usp.* **42**, 165 (1999).  
 [6] M. R. Maxey, *J. Fluid Mech.* **174**, 441 (1987).  
 [7] T. Elperin, N. Kleeorin, and I. Rogachevskii, *Phys. Rev. Lett.* **77**, 5373 (1996).  
 [8] E. Balkovsky, G. Falkovich, and A. Fouxon, *Phys. Rev. Lett.* **86**, 2790 (2001).  
 [9] J. Bec, *Phys. Fluids* **15**, L81 (2003).  
 [10] H. Sigurgeirsson and A. M. Stuart, *Phys. Fluids* **14**, 4352 (2002).  
 [11] J. M. Deutsch, *J. Phys. A* **18**, 1457 (1985).  
 [12] B. Mehlig and M. Wilkinson, *Phys. Rev. Lett.* **92**, 250602 (2004).  
 [13] M. Wilkinson and B. Mehlig, *Phys. Rev. E* **68**, 040101(R) (2003).  
 [14] L. Piterbarg, *SIAM J. Appl. Math.* **62**, 777 (2001).  
 [15] J.-P. Eckmann and D. Ruelle, *Rev. Mod. Phys.* **57**, 617 (1985).  
 [16] Y. Le Jan, *Z. Wahrscheinlichkeitstheor. Verwandte Geb.* **70**, 609 (1985).  
 [17] P. Baxendale and T. Harris, *Ann. Prob.* **14**, 1155 (1986).  
 [18] L. D. Landau and E. M. Lifshitz, *Fluid Mechanics* (Pergamon, Oxford, 1958).  
 [19] U. Frisch, *Turbulence*, (Cambridge University Press, Cambridge, 1997).  
 [20] N. G. van Kampen, *Stochastic Processes in Physics and Chemistry* (North-Holland, Amsterdam, 1992).  
 [21] P. A. M. Dirac, *The Principles of Quantum Mechanics* (Oxford University Press, Oxford, 1930).  
 [22] R. B. Dingle, *Asymptotic Expansions: Their Derivation and Interpretation* (Academic, New York, 1973).